Monthly Notices
of the
ROYAL ASTRONOMICAL SOCIETY

Mon. Not. R. Astron. Soc. **402,** 691–704 (2010) doi:10.1111/j.1365-2966.2009.15927.x

Physical parameters of the Small Magellanic Cloud RR Lyrae stars and the distance scale

Sukanta Deb[1]★ and Harinder P. Singh[1,2]

[1]*Department of Physics & Astrophysics, University of Delhi, Delhi 110007, India*
[2]*CRAL-Observatoire de Lyon, CNRS UMR 142, 69561 Saint-Genis Laval, France*

Accepted 2009 October 23. Received 2009 October 22; in original form 2009 August 8

ABSTRACT

We present a careful and detailed light curve analysis of RR Lyrae stars in the Small Magellanic Cloud (SMC) discovered by the Optical Gravitational Lensing Experiment (OGLE) project. Out of 536 single-mode RR Lyrae stars selected from the data base, we have investigated the physical properties of 335 'normal-looking' RRab stars and 17 RRc stars that have good quality photometric light curves. We have also been able to estimate the distance modulus of the cloud which is in good agreement with those determined from other independent methods. The Fourier decomposition method has been used to study the basic properties of these variables. Accurate Fourier decomposition parameters of 536 RR Lyrae stars in the OGLE-II data base are computed. Empirical relations between the Fourier parameters and some physical parameters of these variables have been used to estimate the physical parameters for the stars from the Fourier analysis. Further, the Fourier decomposition of the light curves of the SMC RR Lyrae stars yields their mean physical parameters as [Fe/H] $= -1.56 \pm 0.25$, $M = 0.55 \pm 0.01\,\mathrm{M}_{\odot}$, $T_{\rm eff} = 6404 \pm 12$K, $\log L = 1.60 \pm 0.01\,\mathrm{L}_{\odot}$ and $M_V = 0.78 \pm 0.02$ for 335 RRab variables and [Fe/H] $= -1.90 \pm 0.13$, $M = 0.82 \pm 0.18\,\mathrm{M}_{\odot}$, $T_{\rm eff} = 7177 \pm 16$K, $\log L = 1.62 \pm 0.02\,\mathrm{L}_{\odot}$ and $M_V = 0.76 \pm 0.05$ for 17 RRc stars. Using the absolute magnitude together with the mean magnitude, intensity-weighted mean magnitude and the phase-weighted mean magnitude of the RR Lyrae stars, the mean distance modulus to the SMC is estimated to be 18.86 ± 0.01, 18.83 ± 0.01 and 18.84 ± 0.01 mag, respectively, from the RRab stars. From the RRc stars, the corresponding distance modulus values are found to be 18.92 ± 0.04, 18.89 ± 0.04 and 18.89 ± 0.04 mag, respectively. Since the Fourier analysis is a very powerful tool for the study of the physical properties of the RR Lyrae stars, we emphasize the importance of exploring the reliability of the calculation of Fourier parameters together with the uncertainty estimates keeping in view the large collections of photometric light curves that will become available from variable star projects of the future.

Key words: methods: data analysis – astronomical data bases: miscellaneous – stars: fundamental parameters – stars: variables: other – Magellanic Clouds.

1 INTRODUCTION

RR Lyrae (RRL) stars have played an important role in determining the cosmic distance scale in modern astronomy. While several studies have used classical Cepheids as primary distance indicators, RRL stars have received substantial attention in solving the distance scale problem. Apart from distance determinations, RRL stars are of particular importance as a test bed for the theories of stellar and galactic structure and evolution. They are the tracers of old stellar populations of the bulge, disc and halo components that are present everywhere. RRL stars are radially pulsating A-F variable stars with periods in the 0.2–1.2 d range and amplitude of variation ≤ 2 mag. They can be easily identified and play a key role as the cornerstone of the Population II distance scale. They are extensively used to determine distances to old and sufficiently metal-poor systems, where they are commonly found in large numbers. In particular, RRL stars are present in globular clusters (GCs) and the dwarf galaxies in the neighbourhood of the Milky Way (Greco et al. 2007), and have also been identified in the M31 field (Brown et al. 2004; Dolphin et al. 2004), in some M31 companions (Pritzl et al. 2005), and in at least four M31 GCs (Clementini et al. 2001). Distances to the Large Magellanic Cloud (LMC) for the Population II objects are based on the luminosity of the RRL stars (Clementini et al. 2002).

★E-mail: sdeb@physics.du.ac.in

There have been very few studies to estimate the distance scale of the Small Magellanic Cloud (SMC) using the RRL stars. Using four RRL light curves of the SMC cluster NGC 121, Walker & Mack (1988) have estimated the distance modulus of the cluster to be 18.86 ± 0.07 mag. On the other hand, using 22 RRL stars surveyed around 1.3 deg^2 near the north-east arm of the SMC field NGC 361, Smith et al. (1992) obtained the distance modulus of the SMC as 18.90 ± 0.16 mag. Also, there are other studies of estimating the distance scale of the SMC based on the binary star light curves and double-mode Cepheids. Harries, Hilditch & Howrath (2003) reported that the distance modulus to the SMC is of the order of 18.89 ± 0.14 mag taking 10 eclipsing binaries in the SMC. By selecting 40 eclipsing binaries of spectral type O and B in the SMC, Hilditch, Howrath & Harries (2005) have derived the fundamental parameters of the binaries and refined the distance modulus to the SMC to 18.91 ± 0.1 mag. Also Kovács (2000) found the distance modulus of the SMC to be 19.05 ± 0.017 mag based on the photometric data of double-mode Cepheids from the Optical Gravitational Lensing Experiment (OGLE) project.

The stellar atmospheric parameters of effective temperature ($T_{\rm eff}$) and surface gravity ($\log g$) are of fundamental astrophysical importance. They are the pre-requisites to any detailed abundance analysis and define the physical conditions in the stellar atmosphere and hence are directly related to the physical properties mass (M), radius (R) and luminosity (L) of the star. In this paper, we present an independent analysis of 536 SMC RRL stars discovered by the OGLE project (Soszynski et al. 2002, hereafter SZ02). The OGLE data base is a very wealthy resource for studying the characteristics of variable stars in the Galaxy, LMC and SMC. For the first time, we make use of the OGLE SMC data to estimate the distance scale of the SMC using a large number of well-sampled RRL light curves. The road map of the present investigation is to perform a Fourier analysis of the RRL stars in order to estimate their physical parameters and hence the SMC distance scale.

We employ the Fourier decomposition (FD) technique which is used extensively to characterize the observed photometric light curves of RRL and other types of variables. The accurate determination of the Fourier coefficients is, therefore, an important task. We have performed an independent automated Fourier analysis of all the RRL light curves selected in this paper by a computer code developed by us. In Section 2, we give a brief description of the data base that we use and the procedure of removing the outliers from the light curve data. We present FD of the light curves in Section 3. We also describe the use of the unit-lag autocorrelation function for finding out the optimal order of the fit to the RRL light curves. Section 4 describes the error analysis of the FD parameters ϕ_{i1} and R_{i1}. Section 5 describes the calibration of the I-band data to the V band. In Section 6, we describe the various physical parameters of the RRLs obtained by using empirical relations from the literature. Section 7 describes the distance determination of the SMC. Lastly, in Section 8, we present the conclusions of our study.

2 THE OBSERVATIONAL DATA BASE

The RRL stars analysed in the present work were selected from the high-quality photometric catalogue of RRL stars in the SMC from OGLE-II data base (SZ02). The catalogue contains B, V and I light curves of 58 RRc stars and 478 RRab stars located in the 11 areas close to the bar of the SMC in the Johnson–Cousins photometric system. The target stars selected for the present analysis were passed through a multipass non-linear fitting algorithm in Interactive Data Language (IDL) which is very efficient in removing the outliers from the data set. Points lying 2σ away from the fit are rejected from the data set so that the objects with well-sampled and accurate light curves are available for the analysis. All the selected targets have evenly covered I-band light curves with about 100–400 data points in I band with an internal accuracy of 0.03–0.13 mag in I band. The B and V light curves in the SZ02 catalogue are of lower quality and have a limited number of data points (20–40). Therefore, we use only the I-band data for estimation of the Fourier parameters. In Figs 1(a) and (c), we show the typical phased light curve of an RRab and an RRc star in the data base. The corresponding light curves with outliers $\geq 2\sigma$ removed are shown in panels (b) and (d), respectively.

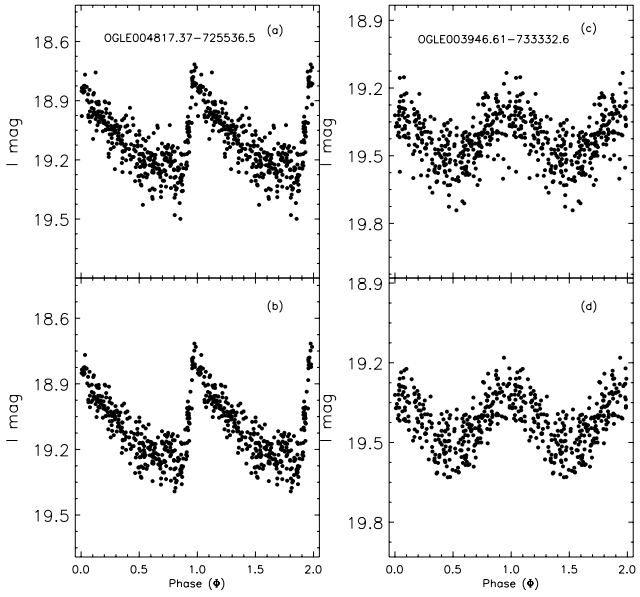

Figure 1. Examples of light curve data from the OGLE-II data base – (a) raw RRab light curve, (c) raw RRc light curve. In panels (b) and (d), the corresponding outlier removed smoothed light curves are shown.

3 FOURIER DECOMPOSITION OF THE LIGHT CURVES

FD technique is a powerful and robust technique for describing the shape of the photometric light curves of the RRL and other variable stars. The method has also been utilized for variable star classification (Deb & Singh 2009), finding the physical parameters of stars like absolute magnitude, metallicity, effective temperature, gravity, helium abundance, etc. of RRL and other stars (Kovács & Kupi 2007, and references therein). The method in its modern form has been revived by Simon & Lee (1981) to describe the progression of Cepheid light curve with increasing period called Hertzsprung progression. They showed that the lower order Fourier parameters are able to completely describe the progression of Cepheid light curves. With theoretical light curves based on hydrodynamical models Simon & Lee (1981), Simon & Clement (1993, hereafter SC93) and Clement & Rowe (2000) were able to derive various physical parameters of stars. On the other hand Kovács and his collaborators (Jurcsik & Kovács 1996, hereafter JK96; Kovács & Jurcsik 1996; Jurcsik 1998; Kovács 1998, hereafter K98; Kovács & Kanbur 1998; Kovács & Walker 1999) were able to estimate astrophysical parameters by establishing empirical relationships between the

Fourier parameters and the physical parameters of stars in the field. A number of studies have made use of these empirical relations to derive the physical parameters of the RRL stars. To list a few of these studies, Kaluzny et al. (2000) used these empirical relations to estimate physical parameters of 26 RRab and 16 RRc stars in M5, Peña et al. (2007) used these empirical relations to estimate physical parameters of seven RRL stars in Bootes and Arellano Ferro et al. (2008) have determined parameters for few RRL variables in NGC 5466. There are a number of other studies that have made use of the Fourier coefficients to determine various parameters of astrophysical importance. Sandage (2004) studied the correlation of particular Fourier components of the light curves of RRab stars with metallicty discovered by Simon and later by Kovács and his co-workers. On the other hand, Morgan, Wahl & Wieckhorst (2006, 2007) have derived empirical relations for RRc stars connecting [Fe/H], period (P) and the Fourier parameter ϕ_{31}. In all the above studies, it has been seen that Fourier parameters can indeed be linked with global stellar parameters such as luminosity, mass, temperature, metallicty and radius. Most of the physical parameter estimations of stars require accurate calculation of Fourier parameters, and any inaccuracies in the determination of Fourier parameters will reflect in the calculated physical parameters of the stars.

We computed FD coefficients for 536 RRL stars in the SMC for the I-band photometric data. The observed magnitudes were fitted with a Fourier cosine series of the form

$$I(t) = A_0 + \sum_{i=1}^{m} A_i \cos[i\omega(t - t_0) + \phi_i], \quad (1)$$

where $I(t)$ is the observed magnitude, A_0 is the mean magnitude, $\omega = 2\pi/P$ is the angular frequency, P is the period of the star in days, t is the time of observation, t_0 is the epoch of maximum light, A_i and ϕ_i are the ith order Fourier coefficients and m is the order of the fit. Equation (1) has $2m + 1$ unknown parameters which require at least the same number of data points to solve for these parameters.

Since period is known from the data base, the observation time can be folded into phase (Φ) as

$$\Phi = \frac{(t - t_0)}{P} - \mathrm{Int}\left[\frac{(t - t_0)}{P}\right].$$

Here, t_0 is the epoch of maximum light of the RRL light curves. The value of Φ is from 0 to 1, corresponding to a full cycle of pulsation and Int denotes the integer part of the quantity. Hence, equation (1) can be written as (Schaltenbrand & Tammann 1971)

$$I(t) = A_0 + \sum_{i=1}^{m} A_i \cos[2\pi i\,\Phi(t) + \phi_i]. \quad (2)$$

The Fourier parameters are defined as

$$R_{i1} = \frac{A_i}{A_1}; \quad \phi_{i1} = \phi_i - i\phi_1,$$

where $i > 1$. The ϕ_{i1} values have been adjusted to lie between 0 and 2π so that they are comparable to those available in the literature.

The optimal order of the fit (m) was chosen to be 4 for RRc stars and 5 for RRab stars by the calculation of unit-lag autocorrelation function (Fig. 2) and looking at the χ^2 value of the fit. A detailed discussion on the optimal order of the fit has been given in Deb & Singh (2009) which involves the calculation of unit-lag autocorrelation function using Baart's condition (Baart 1982; Petersen 1986). Increasing the order of the fit may reduce the χ^2 to some extent, but this will underestimate the distribution. The fits to the phase-folded light curves were made using Levenberg–Marquardt (LM) algorithm which is based on the χ^2-minimization method (Press et al. 1992). The reduced χ^2 for the fit to the RRL light curves are

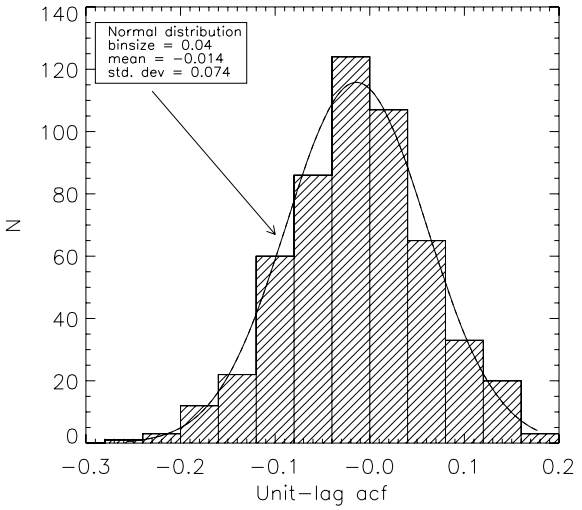

Figure 2. Histogram plot of unit-lag autocorrelation function for 536 SMC RRL stars in the OGLE data base. The order of the fit is 4 and 5, respectively, for the RRc and RRab stars.

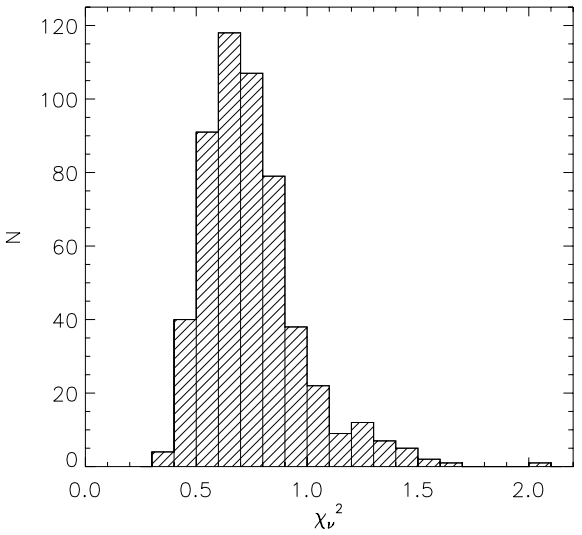

Figure 3. Histogram plot of χ^2_ν of 536 RRL stars selected from the data base.

nearly 1. The histogram plot of the χ^2_ν of the RRL stars is shown in Fig. 3, where ν is the degree of freedom of the fit which is defined as the number of data points minus the number of parameters used to fit the light curve data.

In Figs 4 and 5, we show smoothed (outliers removed) Fourier fitted light curves for 16 randomly selected RRab and RRc stars, respectively. Further, the Fourier parameters for all the stars computed from the I-band data are given in Table 1 (for RRab) and Table 2 (for RRc). N_{obs} denotes the number of data points for each of the light curves retained for the analysis after removing the outliers. D_{m} is the deviation parameter for RRab stars and is discussed in Section 6.1. In Fig. 6, we plot the Fourier amplitude ratios R_{21}, R_{31}, R_{41} and phase differences ϕ_{21}, ϕ_{31}, ϕ_{41} versus log P for the RRL data set. Fig. 7 shows the histogram plot of mean magnitudes (A_0) of all 536 RRL stars.

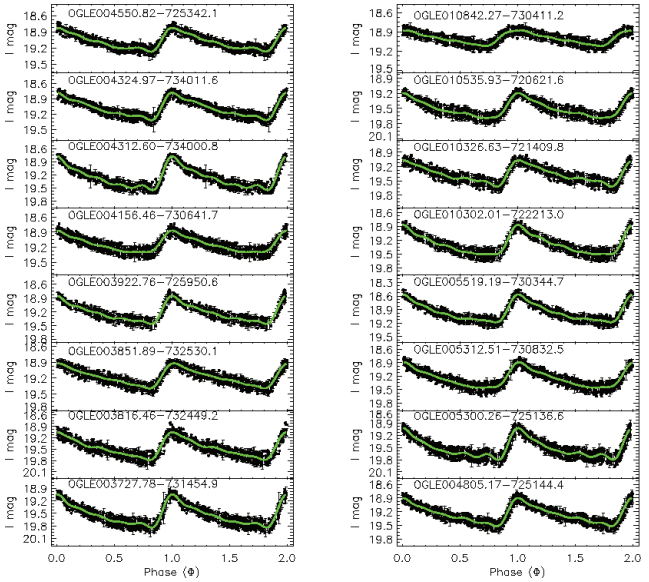

Figure 4. Fourier fitted light curves of a selection of RRab stars after preprocessing of outliers removal. The order of the fit to the light curve is 5. The solid lines show the Fourier fitted light curves.

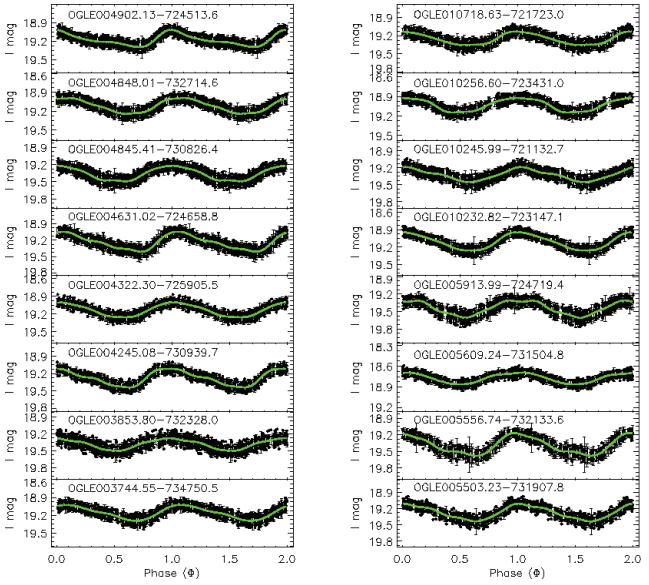

Figure 5. Fourier fitted light curves of a selection of RRc stars after removing the outliers. The order of the fit to the light curve is 4. The solid lines are the Fourier fitted light curves.

4 ERRORS IN THE FOURIER PARAMETERS

The error in $x = f(u, v)$, where the standard errors in u and v are known from the LM method, is given by

$$\sigma^2(x) = {\sigma_u}^2\left(\frac{\partial x}{\partial u}\right)^2 + {\sigma_v}^2\left(\frac{\partial x}{\partial v}\right)^2 + \cdots + 2{\sigma_{uv}}^2\left(\frac{\partial x}{\partial u}\right)\left(\frac{\partial x}{\partial v}\right). \quad (3)$$

In the case of a large number of observations, equation (3) can be reasonably approximated by

$$\sigma^2(x) = {\sigma_u}^2\left(\frac{\partial x}{\partial u}\right)^2 + {\sigma_v}^2\left(\frac{\partial x}{\partial v}\right)^2. \quad (4)$$

Therefore, the errors in R_{i1} and ϕ_{i1} can be approximately written as

$$\sigma_{R_{i1}} = \frac{1}{{A_1}^2}\sqrt{\left(\sigma_{A_1}^2 {A_i}^2 + \sigma_{A_i}^2 {A_1}^2\right)}, \quad (5)$$

$$\sigma_{\phi_{i1}} = \sqrt{{\sigma_{\phi_i}}^2 + i^2{\sigma_{\phi_1}}^2}. \quad (6)$$

In Figs 8 and 9, we plot the distribution of estimated errors in the quantities R_{21}, R_{31}, R_{41} and ϕ_{21}, ϕ_{31} and ϕ_{41}. It is quite obvious that the errors in ϕ_{31} are larger than the errors in ϕ_{21} because the amplitudes for the higher order coefficients are smaller and hence it is very difficult to derive their phase with better precision.

5 CALIBRATION OF THE OGLE SMC RRL DATA SETS

5.1 Fourier parameters in *V* band

The Fourier coefficients of a particular light curve in different photometric bands are different. Non-linear hydrodynamical models have been used by Dorfi & Feuchtinger (1999, hereafter DF99) to obtain *UBVI* light curves of RRL stars. They have computed the inter-relations of the Fourier parameters in V and I bands and compared them with those obtained by Morgan, Simet & Bargenquast (1998, hereafter MSB98) from observed light curves of metal-poor GC M68 by Walker (1994, hereafter W94). However, only eight RRab and eight RRc stars from W94 were used for setting up the relations in MSB98. While the $V - I$ interrelations for amplitude ratios (R_{i1}) of DF99 showed good agreement with the empirical relations of MSB98, large deviations showed up in the relations of some of the phase differences (ϕ_{i1}) for two sets of models with $Z = 0.001$ and 0.0001. DF99 concluded that no distinct metallicity effect could be followed from these results and emphasized the need for more model calculations covering a wide range of stellar parameters.

In order to check the reliability of the theoretical interrelations of the phase parameters of DF99, we have calculated the Fourier phase parameters in the I and V bands from the highly accurate photometric light curves of selected RRab and RRc stars in GC M3 from Benkő, Bakos & Nuspl (2006, hereafter B06) together with the data of eight RRab and eight RRc stars from W94. All the RRab stars free from Blazhko effect and RRc stars having good quality light curves were selected from B06 after visual inspection. We have used 29 RRab variables 1, 6, 9, 25, 27, 31, 32, 42, 53, 57, 58, 69, 84, 89, 93, 94, 100, 109, 135, 137, 139, 142, 144, 146, 148, 165, 167, 175 and 222 of GC M3 from B06 and eight variables 2, 9, 10, 14, 22, 23, 25 and 35 of GC M68 from W94. In the case of RRc stars, 16 variables 21, 37, 75, 86, 88, 107, 126, 128, 131, 147, 152, 171, 177, 208, 213 and 259 of GC M3 from B06 and eight variables 1, 6, 11, 13, 16, 18, 20 and 24 of GC M68 from W94 were used. We call this data set as B06+W94. In Fig. 10, we show the $V - I$ interrelations of the Fourier phase parameters $\phi_{21}, \phi_{31}, \phi_{41}$ for RRab and RRc stars, respectively. Points lying above a threshold sigma ($\sigma_{\rm thres}$) from the fit are rejected using multipass fitting algorithm in IDL . The threshold sigma level is chosen based on a reasonably high degree of correlation between the parameters in the I and V band so that the number of data points for the fit retained are significant. The mean difference of 0.61 per cent in absolute magnitude, 0.23 per cent in log $(L/L_\odot)$, 4.03 per cent in [Fe/H], 0.10 per cent in effective temperature and 1.18 per cent in mass will result when DF99 interrelations are used.

Table 1. Fourier parameters for 478 fundamental mode (RRab) SMC RRL variables in the OGLE data base (*I*- band data).

OGLE ID (1)	Period (2)	N_{obs} (3)	${\chi_\nu}^2$ (4)	σ_{fit} (5)	A_I (6)	A_0 (7)	A_1 (8)	R_{21} (9)	R_{31} (10)	R_{41} (11)	ϕ_{21} (12)	ϕ_{31} (13)	ϕ_{41} (14)	D_m (15)
004801.59-733021.5	0.399 572	292	0.503	0.060	0.821	19.513	0.268	0.504	0.357	0.234	4.105	1.924	0.187	4.737
005300.26-725136.6	0.403 584	306	0.716	0.058	0.786	19.519	0.257	0.561	0.311	0.253	3.785	1.602	5.713	3.860
003841.21-734422.9	0.410 569	289	0.664	0.060	0.843	19.566	0.285	0.468	0.344	0.254	3.888	1.885	6.001	1.195
003727.78-731454.9	0.412 698	286	0.815	0.060	0.799	19.540	0.276	0.463	0.336	0.204	4.116	2.060	0.093	0.356
005728.85-723454.6	0.416 258	229	0.966	0.068	0.765	19.778	0.258	0.469	0.362	0.201	4.344	2.240	0.636	3.282
005728.85-723454.6	0.416 260	229	0.966	0.068	0.765	19.778	0.258	0.469	0.362	0.201	4.344	2.240	0.636	3.282
005629.88-725213.0	0.422 334	233	0.708	0.067	0.258	18.255	0.098	0.471	0.190	0.071	4.310	2.587	6.114	8.038
005026.32-732418.2	0.422 681	314	1.024	0.057	0.630	19.598	0.222	0.469	0.338	0.145	4.164	1.970	6.021	1.151
004639.18-731324.7	0.424 320	301	0.501	0.059	0.873	19.626	0.306	0.468	0.324	0.186	4.053	2.237	0.076	4.716
003816.46-732449.2	0.427 897	291	1.273	0.060	0.734	19.469	0.262	0.519	0.279	0.125	4.367	2.351	0.986	4.522
005110.48-730750.0	0.431 720	303	0.715	0.059	0.879	19.632	0.316	0.459	0.303	0.157	4.249	2.232	0.095	2.621
010134.33-725427.4	0.433 496	291	1.001	0.060	0.645	19.413	0.234	0.440	0.235	0.133	4.165	1.999	5.184	6.134
010452.90-724025.9	0.433 623	267	0.502	0.062	0.580	19.215	0.192	0.455	0.384	0.246	3.910	2.048	6.086	2.635
005719.62-725540.7	0.433 862	254	0.627	0.064	0.747	19.536	0.256	0.530	0.283	0.230	4.080	1.775	0.061	7.359
005646.16-723452.2	0.445 986	269	0.762	0.062	0.774	19.529	0.264	0.460	0.339	0.256	3.823	2.056	0.169	2.242
005957.83-730647.6	0.447 303	256	0.686	0.064	0.784	19.465	0.277	0.447	0.297	0.217	3.913	2.161	0.240	3.408
005458.09-724948.9	0.447 471	275	0.976	0.062	0.663	19.367	0.239	0.345	0.352	0.257	4.128	1.997	0.022	0.201
004758.98-732241.3	0.449 794	299	0.520	0.059	0.764	19.818	0.253	0.484	0.333	0.267	4.059	2.227	0.090	3.250
010535.93-720621.6	0.453 841	255	0.699	0.064	0.498	19.505	0.191	0.503	0.179	0.117	4.094	2.214	6.035	3.863
010516.55-722526.5	0.455 958	256	0.599	0.064	0.756	19.522	0.255	0.498	0.315	0.204	4.267	2.523	0.391	4.913

The complete table is available in the electronic version of this paper (see the Supporting Information).

Table 2. Fourier parameters for 58 overtone mode (RRc) SMC RRL variables in the OGLE data base (*I*-band data).

OGLE ID (1)	Period (2)	N_{obs} (3)	${\chi_\nu}^2$ (4)	σ_{fit} (5)	A_I (6)	A_0 (7)	A_4 (8)	R_{21} (9)	R_{31} (10)	R_{41} (11)	ϕ_{21} (12)	ϕ_{31} (13)	ϕ_{41} (14)
010220.67-723753.6	0.261 244	281	0.599	0.061	0.202	19.611	0.018	0.066	0.142	0.193	6.051	3.361	4.371
010246.69-725030.1	0.262 593	293	0.557	0.060	0.088	18.801	0.012	0.453	0.092	0.319	3.085	4.728	6.096
005609.24-731504.8	0.277 551	265	0.784	0.063	0.173	18.774	0.003	0.103	0.066	0.032	0.250	4.089	1.937
005451.72-723850.4	0.277 966	270	0.642	0.062	0.126	19.027	0.006	0.348	0.285	0.115	4.290	3.298	1.695
005115.64-724739.2	0.280 936	313	0.743	0.058	0.171	19.161	0.011	0.192	0.177	0.128	5.505	3.101	2.957
003908.31-735426.8	0.281 006	297	0.976	0.059	0.153	18.985	0.010	0.306	0.174	0.163	3.717	5.884	5.809
005601.43-724026.2	0.283 717	271	0.713	0.062	0.296	19.584	0.009	0.363	0.075	0.078	4.639	5.659	3.513
005754.46-723248.2	0.283 746	253	0.671	0.064	0.264	18.520	0.004	0.190	0.058	0.033	4.510	5.230	4.612
003706.77-730551.2	0.293 459	292	0.800	0.060	0.141	19.198	0.002	0.236	0.071	0.030	3.767	2.998	0.587
010245.99-721132.7	0.294 040	300	0.717	0.059	0.261	19.326	0.004	0.145	0.140	0.032	4.769	0.719	3.193
004744.89-725530.1	0.297 777	306	0.664	0.058	0.243	19.185	0.010	0.311	0.091	0.088	3.865	0.441	0.843
004633.73-725253.8	0.302 182	293	0.530	0.060	0.260	19.501	0.016	0.123	0.136	0.135	1.416	4.446	3.286
004631.02-724658.8	0.308 220	300	0.459	0.059	0.362	19.241	0.011	0.322	0.096	0.071	4.444	2.469	2.491
003946.61-733332.6	0.309 804	273	0.514	0.062	0.200	19.420	0.008	0.046	0.099	0.080	4.162	1.948	3.494
004902.13-724513.6	0.310 884	314	0.599	0.057	0.282	19.180	0.005	0.541	0.157	0.053	4.196	2.315	6.005
004245.08-730939.7	0.311 416	286	0.739	0.060	0.339	19.277	0.016	0.297	0.031	0.104	4.817	3.105	1.882
005503.23-731907.8	0.313 536	278	1.096	0.061	0.321	19.275	0.011	0.171	0.076	0.075	4.616	2.970	5.392
005913.99-724719.4	0.313 798	252	0.584	0.064	0.305	19.440	0.019	0.078	0.083	0.128	6.105	3.581	5.656
010249.92-720947.1	0.316 409	277	0.518	0.061	0.271	19.379	0.014	0.173	0.039	0.110	4.034	1.202	2.223
004330.74-733416.0	0.320 723	289	0.741	0.060	0.174	19.293	0.002	0.096	0.115	0.021	5.961	2.734	1.187

The complete table is available in the electronic version of this paper (see the Supporting Information).

The Fourier interrelations of the phase parameters from the *I* to the *V* band have the following form:

$$\phi_{i1}{}^V = \alpha + \beta\, \phi_{i1}{}^I. \tag{7}$$

In Tables 3 and 4, we list the interrelations obtained from the B06+W94 data set for RRab and RRc stars. Also given are the theoretical interrelations of DF99. In Fig. 10, we plot the *I*- and *V*-band Fourier parameters. In Fig. 11, we plot the theoretical interrelations between the *I* and *V* bands of DF99 and observational interrelations obtained from the B06+W94 data set.

To compute *V*-band amplitude from *I*-band amplitude, we again resort to the existing work in the literature. In Fig. 12, we plot *V*-band amplitudes as functions of *I*-band amplitudes for RRL stars in four GCs, M68 from W94, IC 4499 from Walker & Nemec (1996), NGC 1851 from Walker (1998) and M3 from B06. Solid

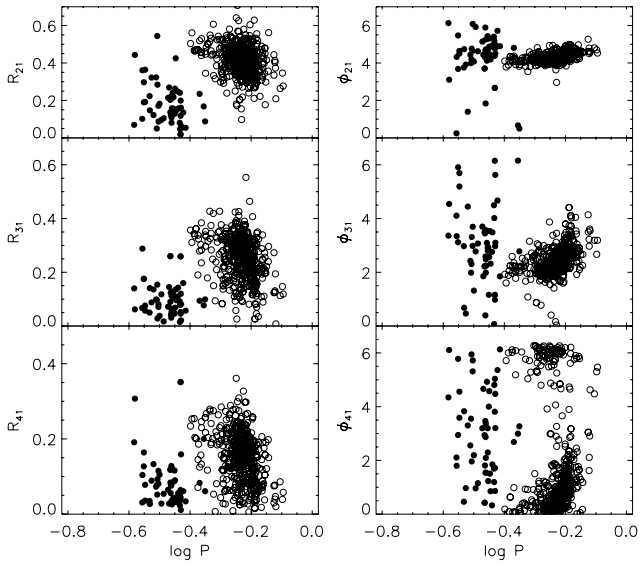

Figure 6. Fourier phase differences ϕ_{21} and ϕ_{31} as a function of log P for the I-band data of 536 program stars. Open circles represent RRab stars and filled circles RRc stars.

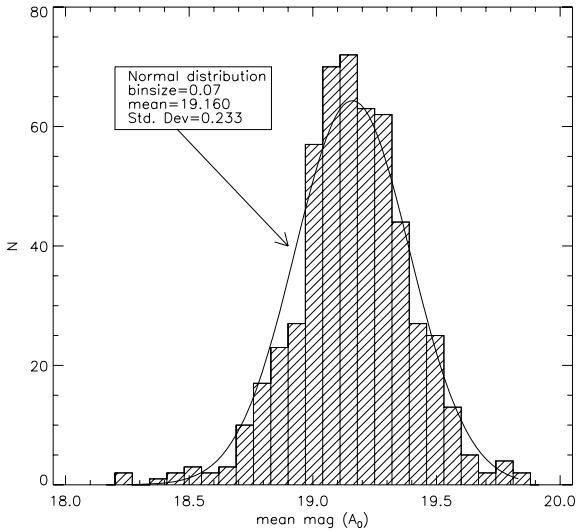

Figure 7. Histogram plot of magnitudes of 536 RRL stars. The solid line is the best-fitting normal distribution.

line denotes the linear relation as determined by a least-squares fit given by

$$A_V = 0.071\,(\pm 0.019) + 1.500\,(\pm 0.040)\,A_I. \quad (8)$$

In Fig. 13, we plot the period–amplitude diagram for all 536 RRL stars.

5.2 Mean magnitudes in V band

Calibration to the standard V-band magnitude is necessary for calculation of the distance scale. The mean magnitude was calculated for each object from its light curve. To transform the I-band mean magnitude to the V band, we used RRL light curves in the V and I bands from the OGLE data base itself. Typical errors in the V-band magnitudes in OGLE are 0.02–0.07 mag. For RRab stars, a linear

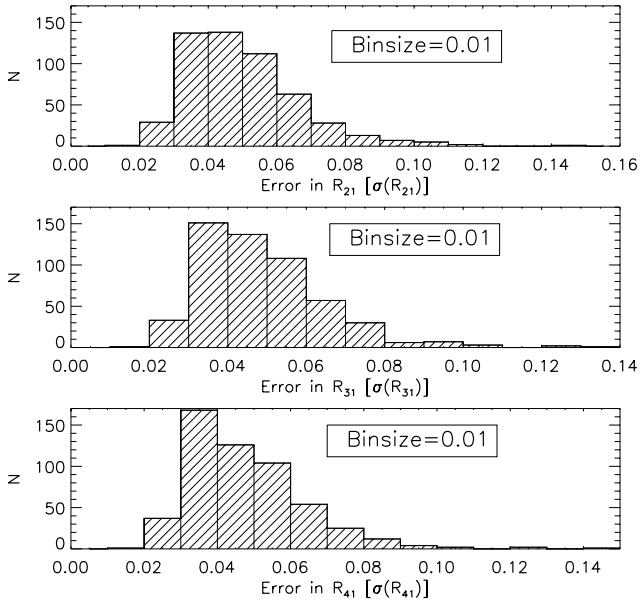

Figure 8. Histogram plot of the distribution of standard errors in R_{21}, R_{31} and R_{41} for the I-band data.

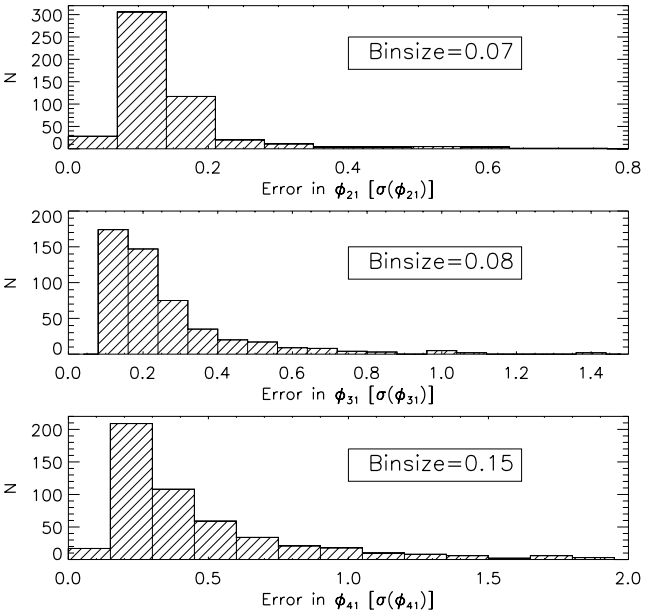

Figure 9. Histogram plot of the distribution of standard errors in ϕ_{21}, ϕ_{31} and ϕ_{41} for the I-band data.

least-squares fit resulted in the following conversion relation:

$$A_0(V) = -0.691\,(\pm 0.029) + 1.068\,(\pm 0.002)\,A_0(I). \quad (9)$$

For the RRc stars, the result of the linear least-squares fit is as follows:

$$A_0(V) = 3.733\,(\pm 0.536) + 0.831\,(\pm 0.028)\,A_0(I). \quad (10)$$

The fits of equations (9) and (10) are shown in Fig. 14. Light curves having mean magnitude variation $\geq 2\sigma$ were discarded and V-band magnitude thus determined. On the other hand, the absolute magnitude calculation of RRab stars required A_1 while RRc stars required A_4 in V band. We used V- and I-band data from W94 and

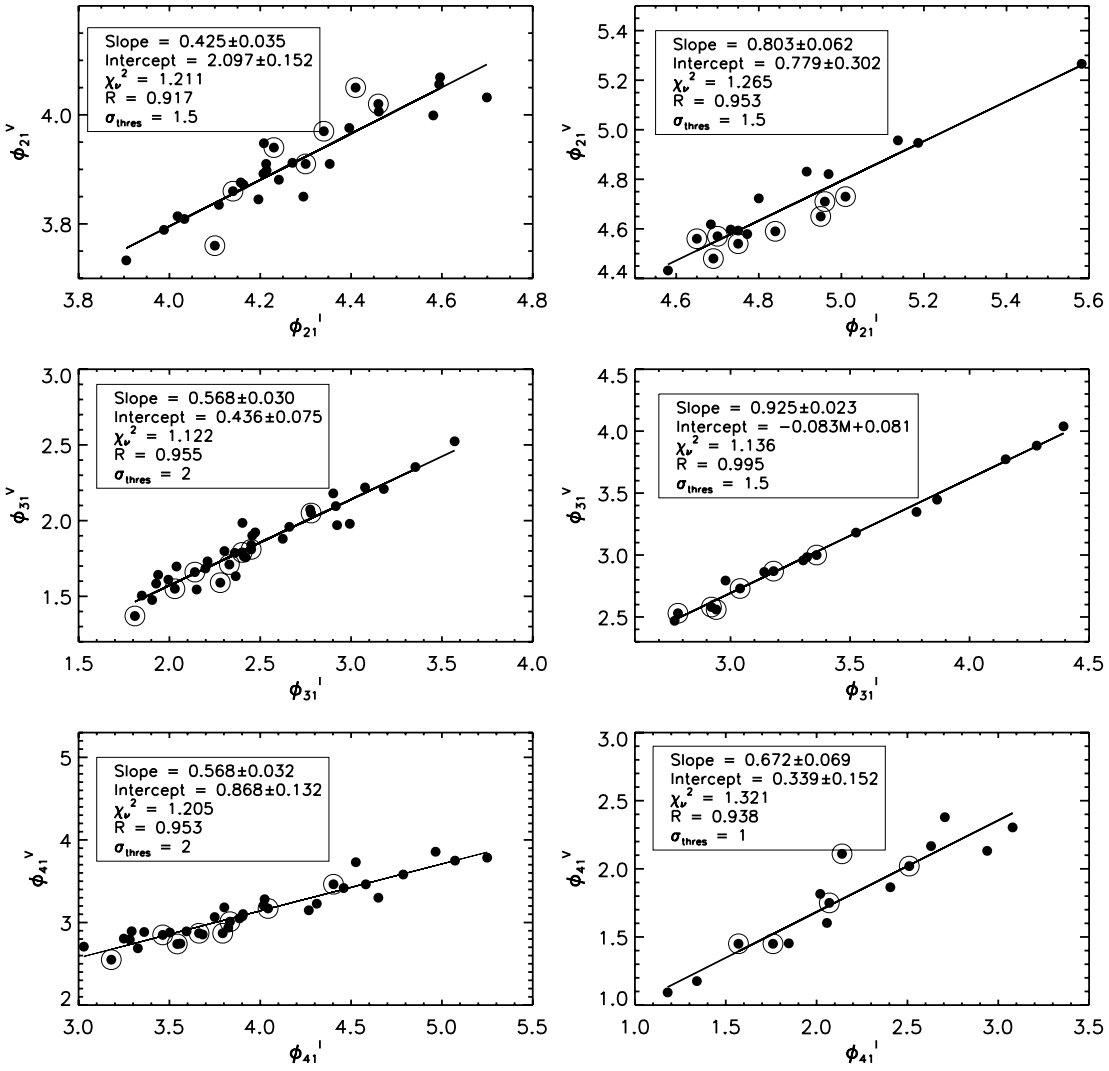

Figure 10. Observational interrelations between *V*- and *I*-band Fourier phase parameters. The left- and right-hand panels show the interrelations for the RRab and RRc stars, respectively. The solid line is the linear fit to the data. The interrelations are based on the cosine series fit. Dots represent the data points from B06 and encircled dots from W94 .

Table 3. Coefficients of the Fourier interrelations for RRab stars from DF99 and B06+W94 data.

Relation	DF99		B06+W94	
	α	β	α	β
$\phi_{21}{}^I \rightarrow \phi_{21}{}^V$	0.693	0.697	2.097 ± 0.152	0.425 ± 0.035
$\phi_{31}{}^I \rightarrow \phi_{31}{}^V$	−0.039	0.788	0.436 ± 0.075	0.568 ± 0.030
$\phi_{41}{}^I \rightarrow \phi_{41}{}^V$	−0.611	0.810	0.868 ± 0.132	0.568 ± 0.033

Table 4. Coefficients of the Fourier interrelations for RRc stars from DF99 and B06+W94 data.

Relation	DF99		B06+W94	
	α	β	α	β
$\phi_{21}{}^I \rightarrow \phi_{21}{}^V$	0.144	0.930	0.779 ± 0.302	0.803 ± 0.062
$\phi_{31}{}^I \rightarrow \phi_{31}{}^V$	−0.249	0.995	-0.083 ± 0.081	0.925 ± 0.023
$\phi_{41}{}^I \rightarrow \phi_{41}{}^V$	−0.305	0.980	0.339 ± 0.153	0.672 ± 0.069

Walker (1998) for the A_4 *V*-band calibration and a linear regression analysis yielded the following relation:

$$A_1(V) = -0.007\,(\pm 0.001) + 1.686\,(\pm 0.040)\,A_1(I) \tag{11}$$

for RRab stars and

$$A_4(V) = 0.001\,(\pm 0.0007) + 1.056\,(\pm 0.115)\,A_4(I) \tag{12}$$

for RRc stars. Following Saha & Hoessel (1990) and Sakai et al. (1999), the intensity-weighted mean magnitudes and phase-weighted mean magnitudes are given by

$$m_{\rm int} = -2.5 \log \sum_{i=1}^{n} \frac{1}{n} 10^{-0.4 m_i}, \tag{13}$$

$$m_{\rm ph} = -2.5 \log \sum_{i=1}^{n} 0.5(\phi_{i+1} - \phi_{i-1}) 10^{-0.4 m_i}, \tag{14}$$

where n is the total number of observations, m_i and ϕ_i are the magnitude and phase of the ith observation, respectively, in order of increasing phase. The intensity-weighted mean magnitude and

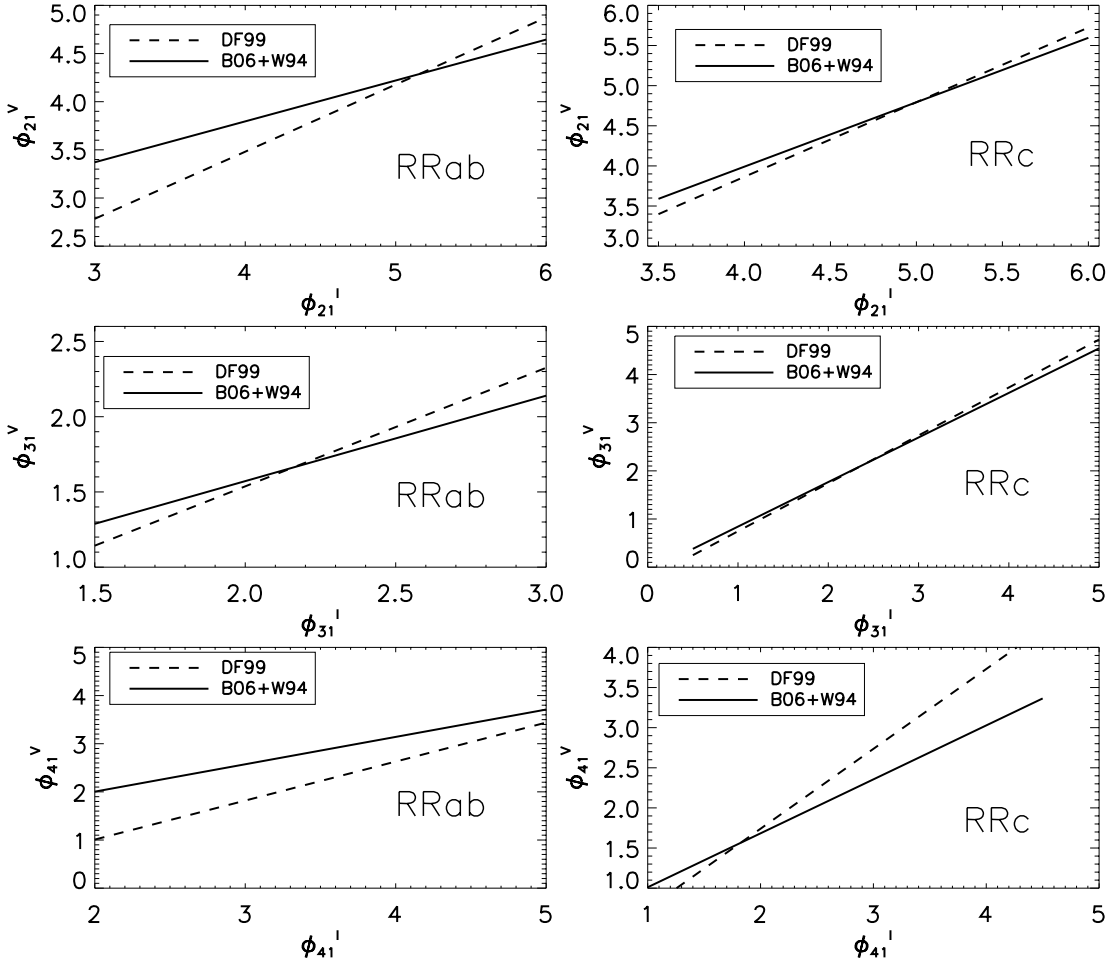

Figure 11. Theoretical interrelations of DF99 between *V*- and *I*-band Fourier phase parameters in comparison with the observational relations calculated from the combined data set of B06 and W94 (B06+W94). The interrelations are based on the cosine series fit.

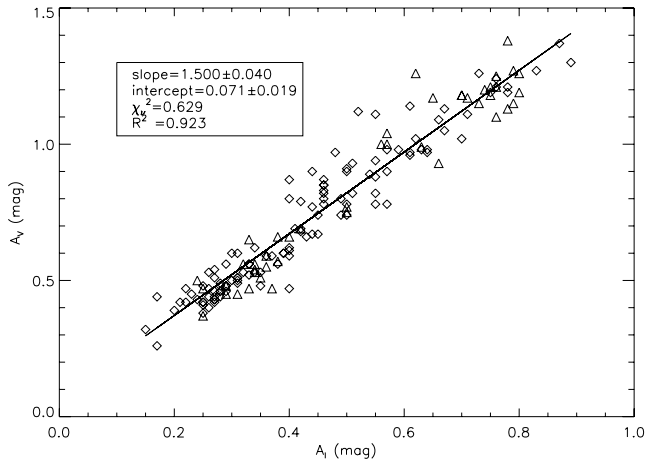

Figure 12. *V*-band amplitudes as functions of *I*-band amplitudes for RRL stars in four GCs. Solid line denotes the linear relation as determined by a least-squares fit. The diamonds denote the observational data taken from W94 (M68), Walker & Nemec (1996) (IC 4499) and Walker (1998) (NGC 1851). The triangles denote the amplitude relations determined by us from the published light curves from B06 (M3). The quadratic correlation coefficient is 0.923.

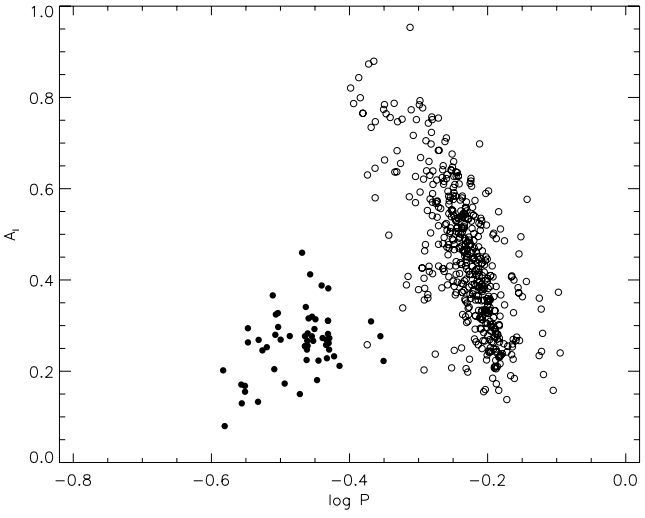

Figure 13. Period–amplitude diagram for all RRab (open circles) and RRc stars (filled circles).

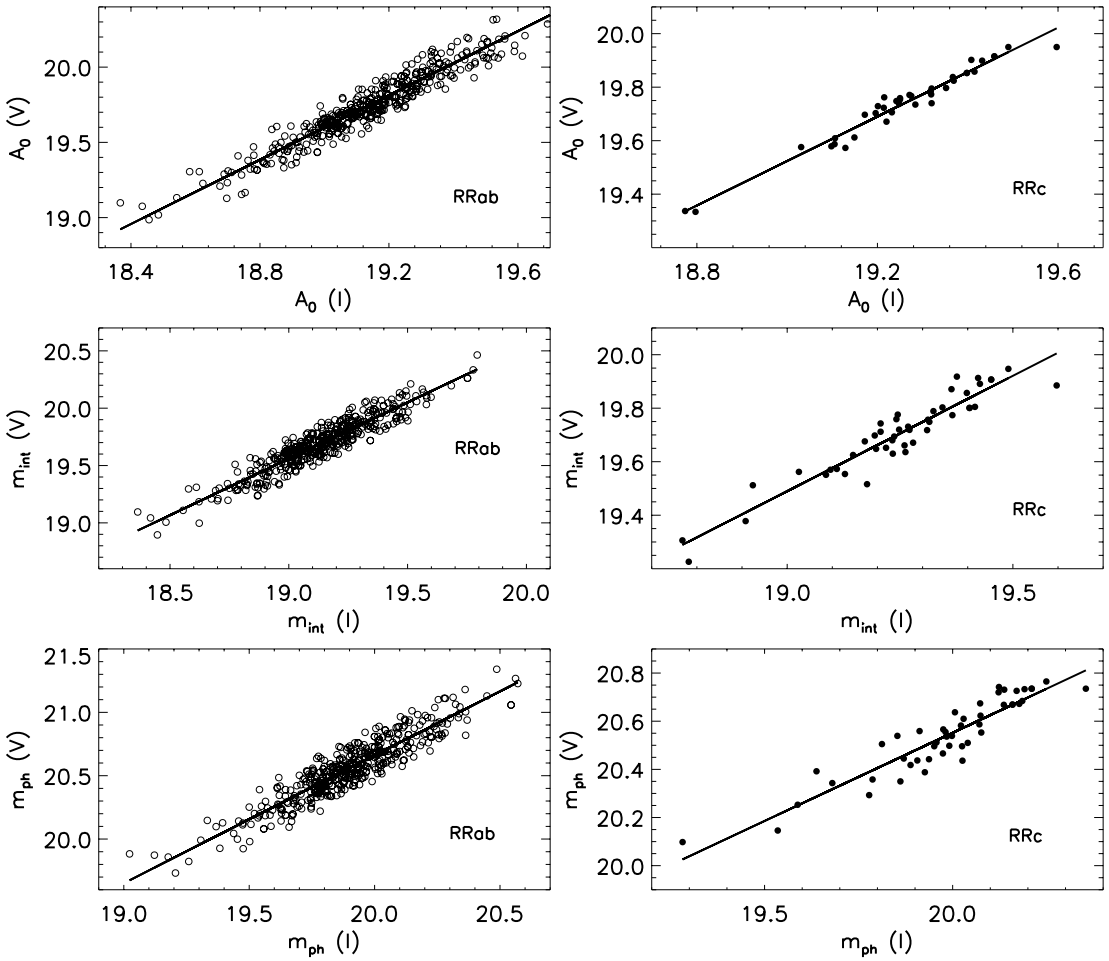

Figure 14. Mean magnitude V-band calibration for RRab stars (open circles) and RRc stars (filled circles). Top panels show fits represented by equations (9) and (10). The lower panels show mean magnitude calibration using both V- and I-band data available for 465 RRab and 55 RRc stars in SZ02.

phase-weighted mean magnitude in the V band have been determined using a linear least-squares fit between the V- and I-band data resulting in the following conversion relations

$$m_{\rm int}(V) = 0.862\,(\pm 0.360) + 0.984\,(\pm 0.019) m_{\rm int}(I), \quad (15)$$

$$m_{\rm ph}(V) = 0.471\,(\pm 0.320) + 1.009\,(\pm 0.021) m_{\rm ph}(I) \quad (16)$$

for RRab stars and

$$m_{\rm int}(V) = 3.093\,(\pm 0.867) + 0.863\,(\pm 0.045) m_{\rm int}(I), \quad (17)$$

$$m_{\rm ph}(V) = 5.900\,(\pm 0.893) + 0.733\,(\pm 0.045) m_{\rm ph}(I) \quad (18)$$

for RRc stars.

6 PHYSICAL PARAMETER EXTRACTION

6.1 RRab stars

Using a set of 81 RRab stars, JK96 derived an empirical relation between the FD parameter ϕ_{31}, period (P) and metallicity [Fe/H] given by

$$[{\rm Fe/H}] = -5.038 - 5.394\,P + 1.345\,\phi_{31}. \quad (19)$$

The Fourier parameters in the above relation were obtained for a sine Fourier series fit. Care has to be taken that the RRab stars to which this equation is applied follow the light curve systematics defined by calibrating the sample of JK96. This can be ensured if the light curve in question satisfies a certain compatibility criterion. The various parameters of the calibrating data set obey well-defined correlations (see table 6 of JK96). Deviation of a light curve from the calibrating characteristics is quantified via the deviation parameter $D_{\rm F}$ defined as

$$D_{\rm F} = \frac{F_{\rm obs} - F_{\rm calc}}{\sigma_{\rm F}},$$

where $F_{\rm obs}$ is the observed value of a given Fourier parameter and $\sigma_{\rm F}$ is the corresponding deviation of various correlations. If the maximum value of $D_{\rm F}$ of each parameter is less than 3 then each light curve satisfies the compatibility condition. This maximum value of $D_{\rm m}$ represents a quality test on the regular behaviour of the shape of the light curve. But, when the test is applied to the RRab stars of OGLE SMC RRL stars some of the stars did not pass this criterion even though the shapes of the light curve are 'normal-looking'. One of the possible reasons is that the OGLE SMC RRL light curves are constructed from the observation in the I band but not in the V band on which the deviation parameter is defined. We have noted that for the deviation parameter up to a value of $D_{\rm m} = 5$, the shapes of the RRab light curves are normal. This value of $D_{\rm m}$ is used as a cut-off limit for the selection of clean samples of RRab stars for analysis.The deviation parameter of individual RRab light curves of the OGLE data has been calculated and

Table 5. Physical parameters extracted from Fourier coefficients for 335 RRab variables.

OGLE ID (1)	M_V (2)	$\log(L/L_\odot)$ (3)	[Fe/H] (4)	$T_{\rm eff}$ (5)	$M/M_\odot$ (6)	$\log g$ (7)	$R/R_\odot(FD)$ (8)	$R/R_\odot$ (Mar) (9)
004801.59-733021.5	0.93 ± 0.02	1.53 ± 0.01	-0.91 ± 0.19	6751 ± 9	0.61 ± 0.01	2.97 ± 0.02	4.27 ± 0.02	4.31 ± 0.03
005300.26-725136.6	0.92 ± 0.02	1.54 ± 0.01	-1.18 ± 0.19	6702 ± 9	0.64 ± 0.01	2.97 ± 0.02	4.40 ± 0.02	4.43 ± 0.03
003841.21-734422.9	0.90 ± 0.01	1.54 ± 0.01	-1.00 ± 0.18	6758 ± 9	0.60 ± 0.01	2.95 ± 0.02	4.33 ± 0.02	4.41 ± 0.03
003727.78-731454.9	0.92 ± 0.01	1.53 ± 0.01	-0.88 ± 0.16	6755 ± 8	0.59 ± 0.01	2.95 ± 0.01	4.29 ± 0.02	4.38 ± 0.02
005728.85-723454.6	0.93 ± 0.02	1.52 ± 0.01	-0.76 ± 0.21	6739 ± 10	0.57 ± 0.01	2.94 ± 0.02	4.26 ± 0.02	4.36 ± 0.03
005728.85-723454.6	0.93 ± 0.02	1.52 ± 0.01	-0.76 ± 0.21	6739 ± 10	0.57 ± 0.01	2.94 ± 0.02	4.26 ± 0.02	4.36 ± 0.03
005026.32-732418.2	0.94 ± 0.02	1.52 ± 0.01	-1.00 ± 0.20	6653 ± 9	0.60 ± 0.01	2.94 ± 0.02	4.39 ± 0.02	4.48 ± 0.03
004639.18-731324.7	0.89 ± 0.02	1.54 ± 0.01	-0.81 ± 0.20	6800 ± 10	0.56 ± 0.01	2.93 ± 0.02	4.29 ± 0.02	4.42 ± 0.03
003816.46-732449.2	0.92 ± 0.02	1.52 ± 0.01	-0.74 ± 0.19	6738 ± 9	0.55 ± 0.01	2.93 ± 0.02	4.29 ± 0.02	4.42 ± 0.03
005110.48-730750.0	0.87 ± 0.01	1.55 ± 0.01	-0.85 ± 0.18	6805 ± 9	0.55 ± 0.01	2.92 ± 0.02	4.33 ± 0.02	4.48 ± 0.03
010452.90-724025.9	0.95 ± 0.01	1.52 ± 0.01	-1.00 ± 0.19	6599 ± 9	0.59 ± 0.01	2.92 ± 0.02	4.44 ± 0.02	4.55 ± 0.03
005646.16-723452.2	0.88 ± 0.01	1.55 ± 0.01	-1.06 ± 0.18	6691 ± 9	0.57 ± 0.01	2.90 ± 0.02	4.48 ± 0.02	4.65 ± 0.03
005957.83-730647.6	0.87 ± 0.01	1.55 ± 0.01	-0.99 ± 0.17	6717 ± 8	0.56 ± 0.01	2.90 ± 0.01	4.44 ± 0.02	4.63 ± 0.03
005458.09-724948.9	0.89 ± 0.01	1.55 ± 0.00	-1.11 ± 0.15	6646 ± 7	0.58 ± 0.01	2.90 ± 0.01	4.51 ± 0.01	4.68 ± 0.02
004758.98-732241.3	0.89 ± 0.02	1.54 ± 0.01	-0.95 ± 0.26	6683 ± 12	0.56 ± 0.01	2.90 ± 0.02	4.45 ± 0.03	4.63 ± 0.04
010535.93-720621.6	0.94 ± 0.02	1.53 ± 0.01	-0.98 ± 0.30	6583 ± 13	0.57 ± 0.01	2.89 ± 0.03	4.49 ± 0.03	4.67 ± 0.05
010516.55-722526.5	0.90 ± 0.02	1.53 ± 0.01	-0.76 ± 0.20	6702 ± 9	0.53 ± 0.01	2.89 ± 0.02	4.38 ± 0.02	4.59 ± 0.03
004721.26-731135.5	0.89 ± 0.01	1.55 ± 0.01	-1.02 ± 0.17	6640 ± 8	0.56 ± 0.01	2.88 ± 0.02	4.52 ± 0.02	4.73 ± 0.03
005504.67-731106.4	0.91 ± 0.01	1.54 ± 0.01	-1.08 ± 0.19	6583 ± 9	0.57 ± 0.01	2.88 ± 0.02	4.56 ± 0.02	4.76 ± 0.03
004306.71-733527.9	0.92 ± 0.02	1.53 ± 0.01	-0.89 ± 0.20	6605 ± 10	0.54 ± 0.01	2.88 ± 0.02	4.49 ± 0.02	4.70 ± 0.03

Note. Errors represent the uncertainties in the Fourier parameters.The complete table is available in the electronic version of this paper (see the Supporting Information).

is given in the last column of Table 1. Cacciari, Corwin & Carney (2005) have also adopted this slightly relaxed criterion to improve the statistics after they verified that this does not lead to any significant difference in the resulting physical parameters. For the RRab analysis, we apply various empirical relations from the literature to all our target stars only when $D_{\rm m} \leq 5$. After implementing this compatibility test, we have found that 355 RRab stars out of 478 are now available for further analysis. This means that our sample of RRab stars now contains 355 RRab stars that have 'normal-looking' light curve shapes. It is also seen that the maximum contribution to the deviation parameter comes from the deviation in ϕ_{31}.

The intrinsic colours as derived from the Fourier parameters of the RRab stars can be used to estimate the temperature of these stars. These colour indices as defined by Jurcsik (1998) are the differences of the magnitude-averaged absolute brightness. The intrinsic colour relation is of the form

$$B - V = 0.308 + 0.163\,P - 0.187\,A_1. \quad (20)$$

The above relation can be used to calculate the effective temperature

$$\log\,T_{\rm eff}\,(B-V) = 3.930 - 0.322\,(B-V) + 0.007\,[{\rm Fe/H}]. \quad (21)$$

The relation between the absolute magnitudes and the Fourier parameters is given by the following relation:

$$M_V = 1.221 - 1.396\,P - 0.477\,A_1 + 0.103\,\phi_{31}. \quad (22)$$

Equation (20) is from Jurcsik (1998) and equation (21) is taken from Kovács & Walker (2001). Equation (22), taken from K98, is based on the relation between the intensity-averaged M_V and the V-band Fourier parameters. On the other hand, on a different absolute scale Jurcsik (1998) derived a relation for the mass of the RRab stars as follows:

$$\log(M/{\rm M}_\odot) = 20.884 - 1.754\,\log\,P + 1.477, \\ \log(L/{\rm L}_\odot) - 6.272\,\log\,T_{\rm eff} + 0.0367\,[{\rm Fe/H}]. \quad (23)$$

The Fourier coefficients in the above equations are based on a sine series fit. But, the coefficients in the present analysis (Table 1) are calculated for a cosine series fit. Therefore, to put the coefficient ϕ_{31} on to the appropriate system, we add 3.145 to ϕ_{31} in Table 1. In Table 5, we list various physical parameters computed from the above empirical relations for 335 RRab stars with regular light curves with $D_{\rm m} \leq 5$. Mean error in the Fourier phase parameter ϕ_{31} for 335 RRab stars is $\sim$0.19. This should result in an uncertainty of $\sim$0.25 dex in [Fe/H], $\sim$0.02 mag in the absolute magnitude, $\sim$12 K in temperature and $\sim$0.01 $M_\odot$ in mass.

6.2 RRc stars

For the RRc stars, we have only retained stars for which the error in ϕ_{31} is less than 0.5. It is generally not desirable to have error larger than 0.2 (Kaluzny et al. 1998). Since the RRc stars in the SMC are fainter and have lower amplitudes, good data for such sources are simply not available at present. Imposing the criterion of $\sigma_{\phi_{31}} < 0.3$ leaves us with only three RRc stars to be used for further analysis. To increase the statistics without significant loss of accuracy, we have chosen $\sigma_{\phi_{31}} < 0.5$ which allows us to analyse 17 RRc stars.

Through hydrodynamical pulsation models, SC93 formulated the following relationships for luminosity, mass and helium abundance (Y) of RRc stars:

$$\log(L/{\rm L}_\odot) = 1.04\,\log\,P - 0.058\,\phi_{31} + 2.41, \quad (24)$$

$$\log(M/{\rm M}_\odot) = 0.52\,\log\,P - 0.11\,\phi_{31} + 0.39, \quad (25)$$

$$\log(T_{\rm eff}) = 3.7746 - 0.1452\,\log\,P + 0.0056\,\phi_{31}, \quad (26)$$

$$\log\,Y = -20.26 + 4.935\,\log(T_{\rm eff}) - 0.2638 \\ \times\,\log(M/{\rm M}_\odot) + 0.3318\,\log(L/{\rm L}_\odot). \quad (27)$$

The rms error to the fit in equation (24) is 0.025.

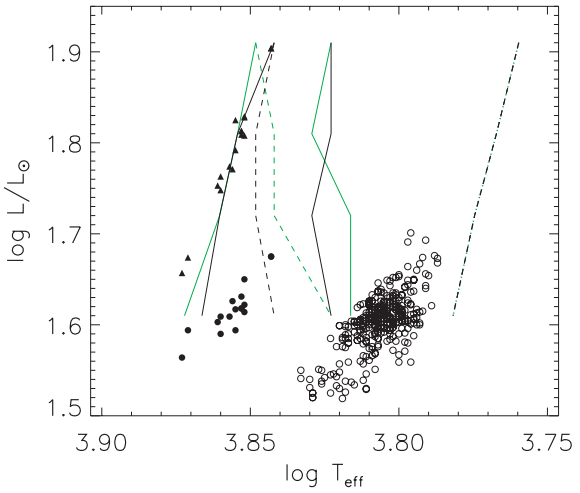

Figure 15. HR diagram of 335 RRab and 17 RRc stars and the theoretical pulsational blue and red edges of the instability strip from Bono et al. (1995). Open circles represent RRab stars, solid circles represent RRc stars with log $(L/\mathrm{L}_\odot)$ calculated from equation (28) and filled upper triangles RRc stars with log $(L/\mathrm{L}_\odot)$ calculated from equation (24). The green solid and dashed lines show the boundaries of the instability strip for RRc and RRab stars, respectively, for mass 0.75 $\mathrm{M}_\odot$, and the black solid and dashed lines show the boundaries of the instability strip for RRc and RRab stars, respectively, for mass 0.65 $\mathrm{M}_\odot$.

Another alternative to equation (24) is the expression for the intensity-averaged absolute magnitude proposed by K98 based on observations of RRc variables in eight different stellar systems:

$$M_V = 1.261 - 0.961\,P - 0.044\,\phi_{21} - 4.447\,A_4, \quad (28)$$

with an rms of 0.042. Kovács derived this formula from the light curves of 106 RRc stars, mainly from Sculptor and M68 and calibrated the zero point from the Baade–Wesselink luminosity scale of Clementini et al. (1995). The phase difference ϕ_{21} in equation (28) is based on a sine series fit. Therefore, 1.571 is subtracted from ϕ_{21} values in Table 2, which are based on a cosine series fit.

Following Lázaro et al. (2006), we have calculated the luminosities of SMC RRc stars from equation (24) as well as from equation (28). The results are plotted in Fig. 15. Luminosities calculated using SC93 relation (equation 24) are larger than those estimated by the K98 relation (equation 28) and the difference may be attributed to different scalings (zero points) of the two relations. The zero point of the luminosity scale of RRc stars is still a matter of controversy (Nemec 2004; Cacciari et al. 2005; Lázaro et al. 2006). Some problems with the Simon's calibration for the RRc stars were also noted by Catelan (2004) who concluded that SC93's relations for L and M cannot both be simultaneously valid. Equations of SC93 (equations 24 and 25) yield

$$\log P = -2.877 + 1.305\,\log(L/\mathrm{L}_\odot) - 0.688\,\log(M/\mathrm{M}_\odot). \quad (29)$$

The above relation lacks a temperature term which should be present according to the period–density relation (Catelan 2004). This is true and remains an unresolved theoretical issue.

The empirical relation for metallicity in terms of the FD parameter ϕ_{31} was derived by Morgan et al. (2007) by considering a large number of stars in different GCs which have the V-band Fourier coefficients available in the literature and the sources of metallicities available for these cluster members. Using the metallicity scales of Zinn & West (1984) and Carretta & Gratton (1997), they obtained the following two empirical relations for RRc stars, respectively,

$$[\mathrm{Fe/H}] = 52.466\,P^2 - 30.075\,P + 0.131\,{\phi_{31}}^2 + 0.982\,\phi_{31} - 4.198\,P\phi_{31} + 2.424, \quad (30)$$

which has a sample standard deviation of 0.145 dex, and

$$[\mathrm{Fe/H}] = 0.034\,{\phi_{31}}^2 + 0.196\,\phi_{31} - 8.507\,P + 0.367, \quad (31)$$

which has a sample standard deviation of 0.142 dex. We have used equation (31) for the calculation of [Fe/H].

The temperatures determined using equation (26) are found to be overestimated for some of the RRc stars. Cacciari et al. (2005) also used equation (26) and found a similar trend for temperature estimates of RRc stars of GC M3 when compared with temperatures derived by Sekiguchi & Fukugita (2000) from the $B - V$ Colours. Temperature differences as large as 500 K have been found for some of the RRc stars. Therefore, the temperature of RRc stars as determined from Fourier coefficients needs to be re-examined. The inaccuracy of the empirical relations connecting the effective temperature, ϕ_{31} term and the period is also reflected in the calculation of the radius of RRc stars. We show ahead that the radii of RRc stars determined from the FD technique differ largely from those determined from the theoretical period–radius–metallicity relation of Marconi et al. (2005). On the other hand, for RRab stars there is a well-matched similarity between the radii determined from the FD technique and from the more fundamental relations used by Marconi et al. (2005). Therefore, the empirical relations derived for the RRab stars seem to be accurate, whereas the physical parameter estimation using the empirical relations derived for the RRc stars may be unreliable. In Table 6, we list the various physical parameters computed from the above empirical relations for the RRc stars with $\sigma_{\phi_{31}} < 0.5$.

Mean error in the Fourier phase parameter ϕ_{31} for 17 RRc stars is ∼0.396. This will result in an uncertainty of ∼0.14 dex in [Fe/H], ∼0.02 in log $(L/\mathrm{L}_\odot)$, ∼ 16 K in temperature and ∼0.18 $\mathrm{M}_\odot$ in mass.

6.3 HR diagram

A Hertzsprung–Russell (HR) diagram of the SMC RRL stars is plotted in Fig. 15 along with the theoretical blue and red edges of the instability strip. The RRc stars are represented by solid circles whereas the RRab stars are represented by open circles. Also shown are the blue and red edges of the instability strip of fundamental (RRab) and first-overtone (RRc) variables derived from the theoretical convective pulsation models of Bono, Caputo & Marconi (1995). It can be easily seen that all the RRab and RRc stars lie well within their instability strips. Although the RRc stars lie inside the instability strip, the empirical relations overestimate the temperatures of these stars.

6.4 Gravity for RRab and RRc stars

From the global physical parameters like mass, luminosity and temperature, the gravity can be calculated from the following equation (cf. Cacciari et al. 2005):

$$\log g = -10.607 + \log(M/\mathrm{M}_\odot) - \log(L/\mathrm{L}_\odot) + 4\log T_{\mathrm{eff}} \quad (32)$$

6.5 Radii of RRLs

The radii of the RRL can be obtained once we know the temperature and the luminosity of the RRL stars using the Stefan–Boltzmann

Table 6. Physical parameters extracted from Fourier coefficients for 17 RRc variables.

OGLE ID (1)	M_V(K98) (2)	$\log(L/L_\odot)$ (SC93) (3)	[Fe/H] (4)	$T_{\rm eff}$ (5)	$M/M_\odot$ (6)	$\log g$ (7)	$R/R_\odot$ (FD) (8)	$R/R_\odot$ (Mar) (9)
005451.72-723850.4	0.85 ± 0.03	1.66 ± 0.02	-1.10 ± 0.17	7457 ± 17	0.59 ± 0.19	3.00 ± 0.33	4.07 ± 0.03	4.19 ± 0.02
005115.64-724739.2	0.78 ± 0.04	1.67 ± 0.02	-1.21 ± 0.16	7425 ± 17	0.62 ± 0.19	3.00 ± 0.31	4.19 ± 0.04	4.25 ± 0.02
010245.99-721132.7	0.83 ± 0.04	1.83 ± 0.03	-2.02 ± 0.11	7165 ± 18	1.13 ± 0.07	3.04 ± 0.06	5.35 ± 0.05	4.63 ± 0.02
004631.02-724658.8	0.78 ± 0.04	1.75 ± 0.03	-1.67 ± 0.17	7266 ± 20	0.77 ± 0.18	2.97 ± 0.24	4.79 ± 0.05	4.65 ± 0.02
004902.13-724513.6	0.82 ± 0.03	1.76 ± 0.02	-1.73 ± 0.13	7247 ± 15	0.80 ± 0.18	2.97 ± 0.23	4.87 ± 0.04	4.69 ± 0.02
010453.59-723756.0	0.78 ± 0.03	1.83 ± 0.01	-2.11 ± 0.08	7115 ± 10	0.93 ± 0.17	2.94 ± 0.18	5.44 ± 0.04	5.09 ± 0.01
010029.57-725454.2	0.77 ± 0.04	1.81 ± 0.02	-2.03 ± 0.09	7136 ± 10	0.85 ± 0.19	2.93 ± 0.22	5.32 ± 0.05	5.10 ± 0.01
010029.57-725454.2	0.77 ± 0.04	1.81 ± 0.02	-2.03 ± 0.09	7136 ± 10	0.85 ± 0.19	2.93 ± 0.22	5.32 ± 0.05	5.10 ± 0.01
004327.25-724542.4	0.76 ± 0.03	1.75 ± 0.02	-1.62 ± 0.13	7238 ± 13	0.64 ± 0.22	2.89 ± 0.34	4.80 ± 0.04	4.96 ± 0.02
010231.17-722134.0	0.69 ± 0.04	1.83 ± 0.03	-2.13 ± 0.15	7107 ± 18	0.91 ± 0.18	2.93 ± 0.19	5.46 ± 0.06	5.16 ± 0.02
005556.74-732133.6	0.77 ± 0.05	1.77 ± 0.03	-1.80 ± 0.17	7193 ± 18	0.70 ± 0.21	2.89 ± 0.31	5.00 ± 0.06	5.07 ± 0.03
003934.35-730433.9	0.76 ± 0.03	1.79 ± 0.02	-1.92 ± 0.13	7161 ± 13	0.76 ± 0.21	2.90 ± 0.28	5.16 ± 0.04	5.13 ± 0.02
010647.29-723053.7	0.73 ± 0.04	1.81 ± 0.02	-2.03 ± 0.13	7124 ± 14	0.77 ± 0.21	2.88 ± 0.27	5.31 ± 0.04	5.27 ± 0.02
005155.37-724909.5	0.73 ± 0.04	1.77 ± 0.02	-1.78 ± 0.17	7183 ± 16	0.65 ± 0.23	2.86 ± 0.35	5.00 ± 0.05	5.19 ± 0.03
010316.37-724816.2	0.66 ± 0.12	1.90 ± 0.03	-2.56 ± 0.13	6968 ± 18	1.14 ± 0.12	2.92 ± 0.11	6.20 ± 0.15	5.54 ± 0.02
010316.37-724816.2	0.66 ± 0.12	1.90 ± 0.03	-2.56 ± 0.13	6968 ± 18	1.14 ± 0.12	2.92 ± 0.11	6.20 ± 0.15	5.54 ± 0.02
005527.97-724136.8	0.76 ± 0.04	1.81 ± 0.03	-2.03 ± 0.16	7118 ± 17	0.75 ± 0.22	2.87 ± 0.29	5.32 ± 0.05	5.35 ± 0.03

Note. Errors represent the uncertainties in the Fourier parameters. This table is also available in the electronic version of this paper (see Supporting Information).

law. Marconi et al. (2005) have recently given a new theoretical period–radius–metallicity relation for the RRLs based on detailed and homogeneous set of non-linear models with a wide range of stellar masses and chemical compositions. We show how the radii obtained by the FD method compare to the radii obtained from the period–radius–metallicity (PRZ) relation of Marconi et al. (2005). For the sake of completeness, their PRZ relations are given as follows:

$$\log R = 0.774(\pm0.009) + 0.580(\pm0.007)\ \log P \\ -0.035(\pm0.001)\ \log Z \quad (33)$$

for RRab stars with $\sigma = 0.008$,

$$\log R = 0.883(\pm0.004) + 0.621(\pm0.004)\ \log P \\ -0.0302(\pm0.001)\ \log Z \quad (34)$$

for RRc stars with $\sigma = 0.004$. $\log Z$ can be calculated from the relation

$$\log Z = [\mathrm{Fe/H}] - 1.70 + \log(0.638 f + 0.362), \quad (35)$$

where f is an α-enhancement factor with respect to iron (Salaris, Chieffi & Straniero 1993). We take $f = 1$. In Fig. 16, we compare our determinations of the radii using the FD technique with those obtained by Marconi et al. (2005) empirical relations (Mar). In case of the radius determinations of RRc stars by the FD method, the SC93's equations for $\log\ L$ and $\log\ T$ are used. It can be seen that the radii obtained by the two different methods are quite consistent for RRab stars. The solid line in Fig. 16 represents the best least-squares fit. The correlation coefficient between the two radii determinations for the RRab stars is 0.994, whereas for the RRc stars (lower panel of Fig. 16) the correlation coefficient is 0.880. This suggests that the radii determinations by the two independent methods are strongly correlated for the RRab stars, whereas this is not the case for the RRc stars.

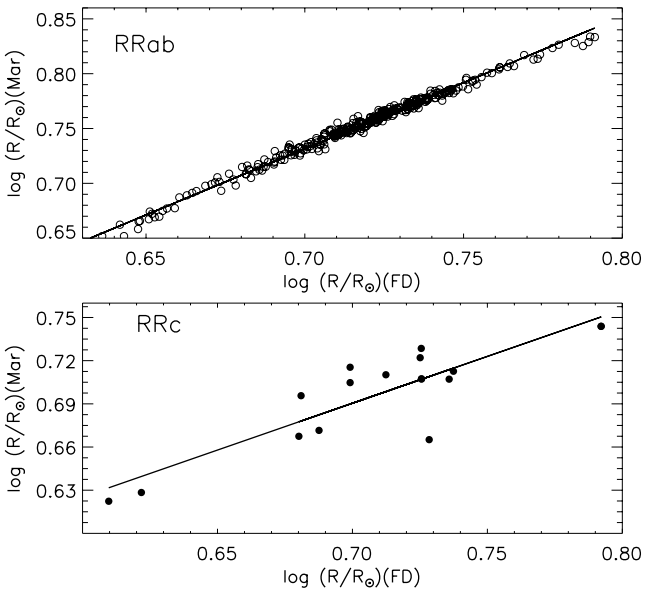

Figure 16. Radii obtained from the empirical relation of Marconi et al. (2005) are plotted versus the radii determined from the FD method. For RRab (open circles) stars in the upper panel, the linear regression analysis yields: $\log(R/R_\odot)(\mathrm{Mar}) = -0.112(\pm0.005) + 1.206(\pm0.007)\ \log(R/R_\odot)$ (FD), and for the RRc stars (filled circles) in the lower panel the linear regression analysis yields: $\log(R/R_\odot)(\mathrm{Mar}) = 0.235(\pm0.064) + 0.651(\pm0.090)$ $\log(R/R_\odot)$ (FD).

7 DISTANCE TO THE SMC

We use mean magnitude $A_0(V)$, intensity-weighted mean magnitude and phase-weighted mean magnitude separately to derive an independent distance modulus to the SMC. The distance modulus for each star is calculated from their values of mean magnitudes and M_V derived from the Fourier parameters. Assuming the reddening estimates of the 11 SMC fields of SZ02 to be accurate, we take average of the reddening values of these fields as the true estimates of $E(B-V)$. Following SZ02 we take the interstellar extinction as $A_V = 3.24\ E(B-V)$. This value of A_V has been used to estimate the reddening free distance modulus of SMC. Using 335 RRab and 17 RRc stars, we find the mean distance moduli of

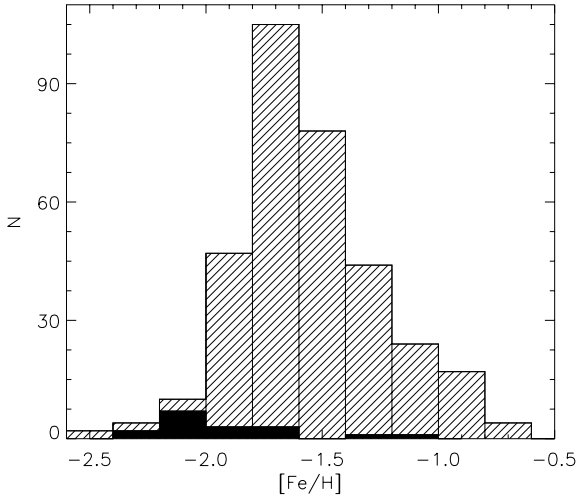

Figure 17. Histogram of the metallicity of the RRLs used for the analysis. The partially filled histogram shows the metallicity distribution of the 335 RRab stars, whereas the fully filled histogram shows the metallicity distribution of the 17 RRc stars.

SMC to be 18.89 ± 0.01, 18.87 ± 0.03 and 18.87 ± 0.02 mag from the mean magnitude, intensity-weighted mean magnitude and phase-weighted mean magnitude, respectively, for all the 352 RRL stars. The uncertainty is the standard deviation of the mean from the individual stars. The mean distance modulus so determined are consistent with the earlier values of 19.05 ± 0.017 (Kovács 2000), 18.89 ± 0.4 (Harries et al. 2003) and 18.91 ± 0.1 (Hilditch et al. 2005).

8 SUMMARY AND CONCLUSIONS

In this paper, we have derived the physical parameters of 352 RRL stars (335 RRab and 17 RRc) of the SMC from OGLE-II I-band data base using the FD of their light curves. The stars were selected based on the quality of their light curves. I-band Fourier coefficients have been converted to V band using the interrelations obtained from the observational data of B06 and W94. Using the FD method, we find the mean physical parameters: [Fe/H] $= -1.56 \pm 0.25$, $M = 0.55 \pm 0.01\,\mathrm{M}_\odot$, $T_{\rm eff} = 6404 \pm 12$ K, $\log L = 1.60 \pm 0.01\,\mathrm{L}_\odot$ and $M_V = 0.78 \pm 0.02$ for 335 RRab variables and [Fe/H] $= -1.90 \pm 0.13$, $M = 0.82 \pm 0.18\,\mathrm{M}_\odot$, $T_{\rm eff} = 7177 \pm 16$ K, $\log L = 1.62 \pm 0.02\,\mathrm{L}_\odot$ and $M_V = 0.76 \pm 0.05$ for 17 RRc stars. Fig. 17 shows the metallicity distribution of the 352 SMC RRL stars used for the analysis. Mean distance modulus to the SMC was calculated from the 352 light curves by using mean magnitude, intensity-weighted mean magnitude and phase-weighted mean magnitude. The values of the distance modulus are found to be in good agreement with independent studies. Locations of the RRL stars in the HR diagram clearly show that the estimates of the parameters determined from the FD method are consistent with the theoretical blue and red edges of the instability strip calculated by Bono et al. (1995). The calculations of the radii of the RRLs by using the FD technique are in agreement with the theoretical period–radius–metallicity relations of Marconi et al. (2005) obtained from a completely different approach of non-linear convective modelling.

ACKNOWLEDGMENTS

SD thanks CSIR, Govt. of India for a senior research fellowship. HPS is grateful to CRAL-Observatoire de Lyon for an invited professorship. Authors thank the reviewer Dr Horace Smith for many useful comments and suggestions which improved the presentation of this paper.

REFERENCES

Arellano Ferro A., Rojas López V., Giridhar S., Bramich D. M., 2008, MNRAS, 384, 1444
Baart M. L., 1982, IMA J. Numer. Analysis, 2, 241
Benkő J. M., Bakos G. Á., Nuspl J., 2006, MNRAS, 372, 1657 (B06)
Bono G., Caputo F., Marconi M., 1995, AJ, 110, 2365
Brown T. M., Ferguson H., Smith E., Kimble R. A., Sweigart A. V., Renzini A., Rich R. M., 2004, AJ, 127, 2738
Cacciari C., Corwin T. M., Carney B. E., 2005, AJ, 129, 267
Carretta E., Gratton R. G., 1997, A&AS, 121, 95
Catelan M., 2004, in Kurtz D. W., Pollard K. R., eds, ASP Conf. Ser. Vol. 310, Variable Stars in the Local Group (IAU Colloq. 193). Astron. Soc. Pac., San Fransisco, p. 113
Clement C. M., Rowe J., 2000, AJ, 120, 2579
Clementini G., Carretta E., Gratton R., Merighi R., Mould J. R., McCarthy J. K., 1995, AJ, 110, 2319
Clementini G., Federici L., Corsi C., Cacciari C., Bellazzini M., Smith H. A., 2001, ApJ, 559, L109
Clementini G. et al., 2002, in Aerts C., Bedding T. R., Christensen-Dalsgaard J., eds, ASP Conf. Ser. Vol. 259, Radial and Nonradial Pulsations as Probes of Stellar Physics (IAU Colloq. 185). Astron. Soc. Pac., San Fransisco, p. 124
Deb S., Singh H. P., 2009, A&A, in press (arXiv:0903.3500)
Dolphin A. E., Saha A., Olszewski E. W., Thim F., Skillman E. D., Gallagher J. S., Hoessel J., 2004, AJ, 127, 875
Dorfi E. A., Feuchtinger M. U., 1999, A&A, 348, 815 (DF99)
Greco C. et al., 2007, ApJ, 670, 332
Harries T. J., Hilditch R. W., Howrath I. D., 2003, MNRAS, 339, 157
Hilditch R. W., Howrath I. D., Harries T. J., 2005, MNRAS, 357, 304
Jurcsik J., 1998, A&A, 333, 571
Jurcsik J., Kovács G., 1996, A&A, 312, 111 (JK96)
Kaluzny J., Hilditch R. W., Clement C., Rucinski S. M., 1998, MNRAS, 296, 347
Kaluzny J., Olech A., Thompson I., Pych W., Krzeminski W., Schwarzenberg-Czerny A., 2000, A&AS, 143, 215
Kovács G., 1998, Mem. Soc. Astron. Ital., 69, 49 (K98)
Kovács G., 2000, A&A, 360, L1
Kovács G., Jurcsik J., 1996, ApJ, 466, L17
Kovács G., Kanbur S. M., 1998, MNRAS, 295, 834
Kovács G., Kupi G., 2007, A&A, 462, 1007
Kovács G., Walker A. R., 1999, ApJ, 512, 271
Kovács G., Walker A. R., 2001, A&A, 374, 264
Lázaro C., Arellano Ferro A., Arévalo M. J., Bramich D. M., Giridhar S., Poretti E., 2006, MNRAS, 372, 69
Marconi M., Nordgren T., Bono G., Schnider G., Caputo F., 2005, ApJ, 623, L133
Morgan S. M., Simet M., Bargenquast S., 1998, Acta Astron., 48, 341 (MSB98)
Morgan S. M., Wahl J. N., Wieckhorst R. M., 2006, Mem. Soc. Astron. Ital., 77, 178
Morgan S. M., Wahl J. N., Wieckhorst R. M., 2007, MNRAS, 374, 1421
Nemec J. M., 2004, AJ, 127, 2185
Peña J. H., Arellano A., Sareyan J. P., Peña R., Alvarez M., 2007, Communications Asteroseismology, 150, 385
Petersen J. O., 1986, A&A, 170, 59
Press W., Teukolsky S., Vetterling W., Flannery B., 1992, Numerical Recipes in FORTRAN, 2nd edn. Cambridge Univ. Press, Cambridge
Pritzl B. J., Armandroff T. E., Jacoby G. H., Da Costa G. S., 2005, AJ, 129, 2232
Saha A., Hoessel J. G., 1990, AJ, 99, 97
Sakai S. et al., 1999, ApJ, 523, 540
Salaris M., Chieffi A., Straniero O., 1993, ApJ, 350, 645
Sandage A., 2004, AJ, 128, 858

Schaltenbrand R., Tammann G., 1971, A&AS, 4, 265
Sekiguchi M., Fukugita M., 2000, AJ, 120, 1072
Simon N. R., Clement C. M., 1993, ApJ, 410, 526 (SC93)
Simon N., Lee A., 1981, ApJ, 248, 291
Smith H. A., Silbermann N. A., Baird S. R., Graham J. A., 1992, AJ, 104, 1430
Soszyński I. et al., 2002, Acta Astron., 52, 369 (SZ02)
Walker A. R., 1994, AJ, 108, 555 (W94)
Walker A. R., 1998, AJ, 116, 220
Walker A. R., Mack P., 1988, AJ, 96, 872
Walker A. R., Nemec J. M., 1996, AJ, 112, 2026
Zinn R., West M. J., 1984, ApJS, 55, 45

SUPPORTING INFORMATION

Additional Supporting Information may be found in the online version of this article:

Table 1. Fourier parameters for 478 fundamental mode (RRab) SMC RRL variables in the OGLE data base (*I*-band data).

Table 2. Fourier parameters for 58 overtone mode (RRc) SMC RRL variables in the OGLE data base (*I*-band data).

Table 5. Physical parameters extracted from Fourier coefficients for 335 RRab variables. Errors represent the uncertainties in the Fourier parameters.

Table 6. Physical parameters extracted from Fourier coefficients for 17 RRc variables. Errors represent the uncertainties in the Fourier parameters.

Please note: Wiley-Blackwell are not responsible for the content or functionality of any supporting materials supplied by the authors. Any queries (other than missing material) should be directed to the corresponding author for the article.

This paper has been typeset from a TEX/LATEX file prepared by the author.